WIMAGINE: Wireless 64-Channel ECoG Recording Implant for Long Term Clinical Applications

Corinne S. Mestais, Guillaume Charvet, Fabien Sauter-Starace, Michael Foerster, David Ratel, and Alim Louis Benabid

***Abstract*—A wireless 64-channel ElectroCorticoGram (ECoG) recording implant named WIMAGINE has been designed for various clinical applications. The device is aimed at interfacing a cortical electrode array to an external computer for neural recording and control applications. This active implantable medical device is able to record neural activity on 64 electrodes with selectable gain and sampling frequency, with less than 1 μV_{RMS} input referred noise in the [0.5 Hz – 300 Hz] band. It is powered remotely through an inductive link at 13.56 MHz which provides up to 100 mW. The digitized data is transmitted wirelessly to a custom designed base station connected to a PC. The hermetic housing and the antennae have been designed and optimized to ease the surgery. The design of this implant takes into account all the requirements of a clinical trial, in particular safety, reliability, and compliance with the regulations applicable to class III AIMD. The main features of this WIMAGINE implantable device and its architecture are presented, as well as its functional performances and long-term biocompatibility results.**

***Index Terms*—Active implantable medical device (AIMD), brain–computer interface (BCI), ElectroCorticoGrams (ECoG), neural interface, neural prosthesis.**

I. Introduction

THE brain's spontaneous electrical activity is usually recorded from multiple electrodes placed on the scalp over a short period of time, usually 20–40 minutes, known as electroencephalogram (EEG). EEG recording devices are widely used in neurology, in the case of epilepsy. Neurofeedback remains an important extension and is attempted as the basis of brain–computer interfaces (BCI). BCI technology has been used for rehabilitation after stroke and there are a number of reports involving stroke patients in BCI-feedback training. Most publications have demonstrated the efficacy of BCI technology in post-stroke rehabilitation using output devices such as functional electrical stimulation, robots, and ortheses [1]. EEG recording is safe but requires the user to wear a non-ergonomic EEG helmet, necessitates daily repositioning and recalibration, and the signal quality is not sufficient for some of the addressed applications.

Manuscript received July 30, 2013; revised January 16, 2014; accepted May 24, 2014. Date of publication June 30, 2014; date of current version January 06, 2015. This work was supported in part by grants from the French National Research Agency (ANR-Carnot Institute), Fondation Motrice, Fondation Nanosciences, Fondation de l'Avenir, and Fondation Philanthropique Edmond J. Safra.

The authors are with CEA-LETI-CLINATEC, MINATEC Campus, Grenoble, France (e-mail: corinne.mestais@cea.fr).

Color versions of one or more of the figures in this paper are available online at http://ieeexplore.ieee.org.

Digital Object Identifier 10.1109/TNSRE.2014.2333541

As part of an evaluation for epilepsy surgery, it may be necessary to insert electrodes near the surface of the brain via a craniotomy, for a limited period of time. The existing electrocorticographic (ECoG) signal recording devices are not wireless, which is a constraint for the patient. Recently ECoG recordings were used for BCI experiments, based on subdural electrodes [2]–[7], or on epidural electrodes on nonhuman primates [8]. A number of recent studies have shown that ECoG signals from the motor cortex in the 70–160 Hz range show strong encoding of actual and imagined motor activity [9]–[12]. Similar ECoG activations have been successfully used for one- and two-dimensional BCI control in subjects with epilepsy [3], [13].

These implanted ECoG recording electrode arrays are less sensitive to artifacts, offer higher frequency and spatial resolution than EEG and are less invasive than microelectrode arrays. Nevertheless, they are approved for short term applications.

Microelectrodes are exquisitely sensitive tools to record spikes and local field potentials, avoiding low signal to noise ratios and high impedances encountered in EEG. Single-unit recordings have performed successfully in BCI experiments in the laboratory [14]–[17], enabling closed-loop control of a computer cursor [18], [19] and a robotic arm [20]. Despite encouraging successes in clinical applications of these methods [21], single-unit recordings have yielded limited success outside of the laboratory, mainly due to unsolved problems regarding the long-term robustness of the recorded signals [22]–[24]. Fully implantable devices based on microelectrode arrays are under development for animal studies [25].

The choice of cortical grids to record ECoG is a good compromise since it provides significantly better signal quality (better spatial resolution and better signal to noise ratio) than EEG and presents fewer side effects than microelectrode arrays. Again, fully implantable devices are under development [26], [27].

It is important to notice that most of the studies using implanted devices have been limited to short-term experiments in patients temporarily implanted with electrode arrays prior to epilepsy surgery and only a few use interfaces dedicated to the sole purpose of BCI. This is of course related to the technical challenges intrinsic to long-term active implantable medical devices (AIMD).

To address this challenge, CEA/LETI/CLINATEC is currently conducting a project to develop a long-term implantable medical device for real-time recording and wireless transmission of the ECoG signals from each of 64 electrodes available to an external computer housing the control software.

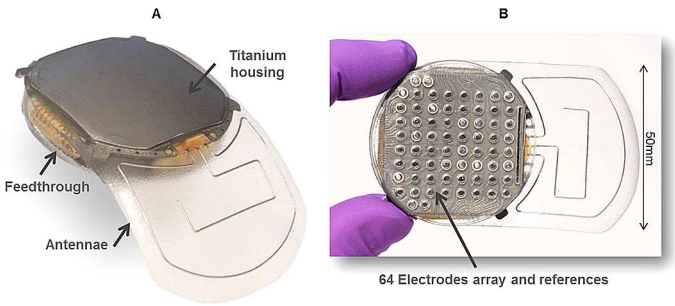

Fig. 1. WIMAGINE ECoG recording implant: A. top and B. bottom view.

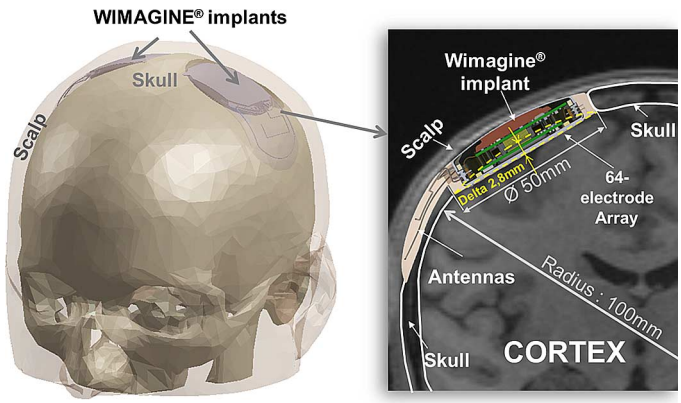

Fig. 2. Surgical placement of the WIMAGINE implant inside a 50-mm craniotomy.

II. Material and Methods

The WIMAGINE (Wireless Implantable Multi-channel Acquisition system for Generic Interface with NEurons) device was developed for recording ECoG signals on 64 electrodes for long-term human implantation.

This AIMD consists of a 50-mm diameter silicone-coated titanium cylinder with a flat internal surface and a silicone-platinum electrode array for ECoG recording. The external surface is convex with a radius of curvature equivalent to the mean MRI skull measurement from several subjects. Its upper surface is in contact with the skin and is used as a neutral electrode, the silicone over-molding (on the rest of the implant) is continuous with an extension containing a HF antenna for transcutaneous remote power supply and an UHF antenna for wireless data transfer (Fig. 1).

The design of the device (patent pending) eases the surgical procedures and ensures safety for the patient. The titanium implant is inserted into a 50-mm craniotomy by the surgeon so that the electrode array is in contact with the dura mater (Fig. 2). The electrode array is composed of 64 biocompatible recording electrodes and three reference electrodes. The set of antennae is made of a medical grade silicone cap placed between the skull and the scalp, therefore avoiding any connector through the skin. Thanks to the wireless connection and remote power supply, the WIMAGINE device is entirely implantable, removing any risk of postoperative infection and facilitating the surgical procedure.

The interface between the brain (soft and not flat) and WIMAGINE's internal surface (solid and flat) could induce pressure in some area of the brain surface. Nevertheless, the drawing below shows that the curvature mismatch of the device with respect to the brain is in the range of 2.8 mm.

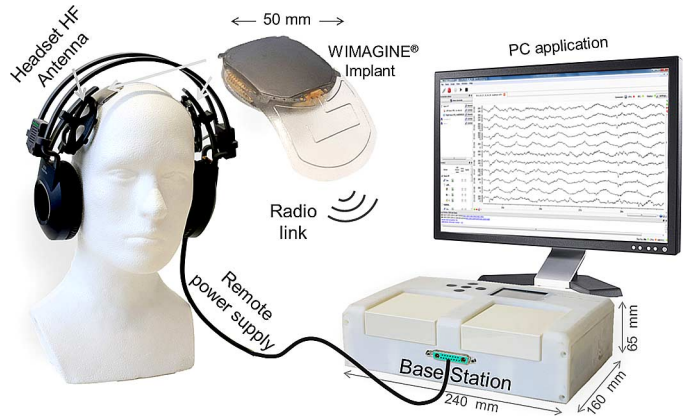

Fig. 3. ECoG recording setup with WIMAGINE Implant.

The WIMAGINE implant records ECoG signals of up to 64 electrodes and transmits wirelessly the raw ECoG data to a computer over a proprietary UHF link in the Medical Implant Communication Service (MICS) band using a custom protocol (Fig. 3). The data analysis and feature extraction is performed on the PC in order to provide maximum flexibility for the signal processing. The system is powered entirely remotely through an inductive link able to provide safely up to 100 mW to the implanted electronics by the means of an external antenna, placed on an audio type helmet, and a field generator.

The design of the WIMAGINE implant takes into account all the constraints of long term implantable medical devices: ultra-low power, miniaturization, safety and reliability. WIMAGINE has been designed to satisfy the Essential requirements of the European Medical Device Directives 93/42/CEE and 90/385/EEC. A risk analysis according to ISO 14971 standard has been conducted in partnership with consultants on regulatory affairs, and risk management actions were set up.

A. Implanted Electronics

The electronic architecture of the implant was designed to be modular and scalable. As a first proof of concept it was therefore chosen not to embed all the functionalities required for an ECoG recording implant into an application specific integrated circuit (ASIC) but rather to use as many off-the-shelf components as possible. Moreover, it was decided to separate functionalities as much as possible in order to request as little redesign as possible for future generations.

1) Design Constraints and Architecture: The electronic requirements for an ECoG recording implant are closely related to the targeted ECoG signal characteristics: in our case the targeted signals have a [0.5 Hz–300 Hz] bandwidth and a [5 μV–3 mV] amplitude [28], [29], when recorded through a platinum electrode array detailed in Section II-C.

In order to expand the range of possible applications (epilepsy recording, BCI recording, etc.) no signal processing functionality was embedded into the designed implant but it was rather decided to transmit the raw recorded signals in real time to a computer where the analysis or recording is performed.

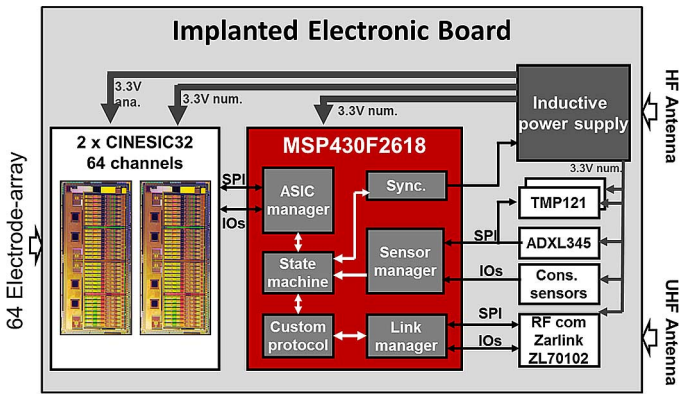

Fig. 4. Block diagram of the electronics of WIMAGINE implant.

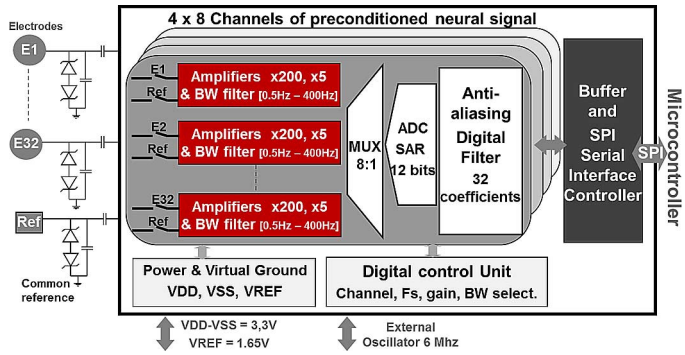

Fig. 5. ASIC CINESIC32 block diagram and external components.

Embedding a high throughput communication feature into an implantable electronic architecture hugely constrains the power budget for the remaining functionalities. As an ultra-low power component for recording low amplitude, low noise signals was not available commercially, it was decided to design an application specific circuit for ECoG recording. This ASIC, the CINESIC32 (CIrcuit for NEural SIgnal Conversion) is able to amplify and digitize 32 channels with an input referred noise of less than 0.7 μV_{RMS} in the [0.5 Hz–300 Hz] range and is detailed in Section II-A2a.

The implant is powered entirely remotely through an inductive link at 13.56 MHz. In order to respect the modular architecture and simplify the developments of future generations where a battery may be embedded, it was decided to use a separate link for the communication between the implant and the PC. The MicroSemi ZL70102 was chosen as it offered the best throughput/power consumption ratio and a custom high level communication protocol was implemented in order to maximize throughput and data reliability as detailed in Section II-B.

These main components as well as several sensors are implemented in the architecture of the implant as described in Fig. 4.

2) Main Components:

ASIC CINESIC32: The targeted neural signals ([5 μV–3 mV], [0.5 – 300 Hz]) are amplified and digitized with very low noise before being transmitted to the PC. The CINESIC32 ASIC is a low power, low noise amplifier that has been specifically designed for ECoG recording with the constraints of implantable applications in mind. The chip was fabricated in AMS 0.35 μm CMOS process and its surface is 89 mm^2. Its characteristics have been detailed elsewhere and compared to other work [30], [31]. The main features of the CINESIC32 include the ability to record with selectable gain (up to x1370), selectable frequency (up to 3k Hz) on any combination of electrodes among its 32 channels and to transmit the 12 bit digitized data over an SPI link to a microcontroller. The acquired data exhibits a very low input referred noise of less than 0.7 μV_{RMS} in the [0.5 Hz – 300 Hz] band at maximum gain and for a sampling frequency of 976 Hz.

The first stage of the ASIC uses a differential input, with high-pass function to suppress the offset voltage due to electrochemical potentials at the electrode-to-body interface (Fig. 5). The ECoG measurement is applied between E_{in} connected to one of the 64 electrodes available and E_{ref} connected to the three reference electrodes of the electrode array. The V_{ref} signal positioned at 1.65 V ($(V_{DD} + V_{SS})/2$) is connected to the titanium housing potential.

Moreover, the CINESIC32 includes programmable analog low pass filters for each channel, as well as a digital low pass FIR filter. In the WIMAGINE implant, two CINESIC32 have been interfaced in order to provide access to 64 recording electrodes. Each electrode is protected by an external capacitor in order to protect the patient of any dc leakage current in a first default condition, as requested by EN 45502–1 [32]. A Zener diode connected to each electrode protects the ASIC of external ESD and a filtering capacitor acts as EMI protection as shown in Fig. 5.

UHF Communication: The wireless transmission of the raw recorded neural signals requires a high throughput of approximately 400 kb/s for the transmission of 32 channels sampled at 976 Hz on 12 bits. Only very few commercially available components offer a high throughput for very low power consumption, the MicroSemi ZL70102 was chosen as it offered an energy per bit of less than 21 nJ and a maximum payload throughput of up to 500 kb/s [33]. Moreover, the ZL70102 has been designed for implantable applications and uses the MICS band in the 400 MHz range where the link budget is less affected by the human body than more conventional links in the 2.45 GHz range. The low level communication protocol is handled by the ZL70102. A custom communication protocol reducing the header/payload ratio has been implemented taking advantage of the low level MAC features of the ZL70102. The designed protocol includes two channels: one low throughput/high data integrity channel with a bit error rate of 10^{-14} for control and command purposes where the configuration commands for the implant are exchanged and a high throughput channel with a BER of $1.5 * 10^{-10}$. Using a custom platinum antenna (detailed in Section II-D2) transmission rates of up to 450 kb/s could be achieved at a distance of up to 2 m. This short range is not an issue since the base station, which also supplies the power to the implant, is small in size and can be easily embedded in the environment of the patient. The overall latency of the designed system, (the time necessary for acquiring a sample and transmitting it to a PC) is less than 30 ms.

For the case where two implants will be used simultaneously on the same patient, the headset may hold two close range antennae placed face to face with the implanted antennae. This

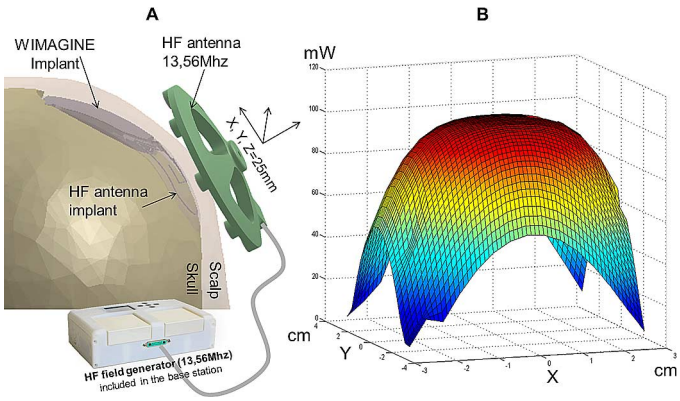

Fig. 6. Placement of the remote power supply antennae and plot of the received power over the inductive link for a distance of 25 mm. A. Setup. B. Results: power received over the inductive link for a distance of 25 mm.

TABLE I
POWER CONSUMPTION FOR IMPLANT COMPONENTS

	Device state			
Consumption (in mW)	***Standby[a] (disconnected)***	***Connected to base station***	***16-channel acquisition[b]***	***32-channel acquisition[b]***
MSP430	9.6	9.6	16.8	36.0
ZL70102	0.0	16.5	18.2	19.8
Analog front end[c]	1.3	7.5	12.5	15.5
Whole device	11.3	33.9	47.9	72.1

a. As the device is not battery powered standby power has not been optimized
b. Sampling frequency: 976Hz; gain: 1370
c. Includes voltage reference and ASIC clock source

provides the advantage of suppressing any interference from devices placed between the implant and the base station. Most importantly, it allows communicating simultaneously with two implants within the MICS band, which is not possible at a distance of 2 m because of the crosstalk of channels in the MICS band.

The bottleneck of the WIMAGINE acquisition system is the wireless data rate. Therefore, the most relevant electrodes are selected for ECoG recording and transmission. Either up to 32 channels can be transmitted with a sampling frequency of 1 kHz or up to 64 channels with a sampling frequency of 600 Hz. In any case, the maximum power consumption is 75 mW.

Inductive Power Supply: Even though the WIMAGINE implant is low power focused, the state of the art batteries only provide power densities several orders of magnitudes lower than what would be required to ensure continuous communication with a PC over the lifespan of the implant. Hence it was decided to entirely power the WIMAGINE implant through an inductive link without any embedded battery. This approach has the advantage of reducing the risk of heat increase during the battery recharge and the time to market of the implant, as regulatory requirements for long term implantable batteries are challenging (IEC-62133). However, as the communication function is completely separated from the power supply, including a rechargeable battery in later developments will not require a complete redesign. The designed inductive link at 13.56 MHz can safely provide up to 100 mW to the implant over up to 25 mm, as shown in Fig. 6.

This inductive power supply has been designed in compliance with European recommendations for inductive applications (ERC7003) and for human exposure to EM fields (CE519). Details of the power consumption for the different components of the implant are given in Table I.

A very rudimentary one-way communication function has been implemented on the inductive link using an RFID protocol. It allows the implant to send a little information at low throughput to the base station and has two purposes. While the inductive helmet is being placed on the patient's head, the implant sends continuous information about the power it receives which allows the operator to place the helmet in the optimum position. Once the implant is recording ECoG activity, the RFID type messages are sent periodically to the base station and provide the necessary information to a synchronization algorithm [34]. This algorithm allows one or two implants to be perfectly synchronized with the base station they are connected to. The brain activity from both hemispheres can therefore be related to external triggers connected to the base station and analyzed synchronously. Thanks to this synchronization mechanism (patented), the WIMAGINE implant can be used with any standard BCI algorithm, even those requiring a tethered connection to external cues like visual or cognitive evoked potentials.

Sensors and Embedded Software: In order to provide additional information about the state of the implant, several sensors are included in the design. An accelerometer (ADXL345) gives information about the position of the patient and may be used to remove artefacts, two temperature sensors (TMP121-EP) monitor the internal temperature of the implant and send warnings to the PC in case a threshold is crossed. Finally, two current sensors measure the current used by the device and the current available through the inductive link, which allows adapting the field generated by the external antenna to the minimum power necessary for proper operation.

In order to manage the two CINESIC32 ASICs, the sensors, the UHF communication link and the inductive power supply, the MSP430F2618 was chosen. The embedded firmware running on this low power microcontroller maximizes the use of the low power modes of the MSP430, thus reducing power consumption, is remotely upgradable and has been designed in compliance with IEC 62304.

3) Electronic Boards: The electronic boards have been designed to fit into a cylindrical titanium housing (diameter 50 mm, height 12.54 mm). As shown in Fig. 7, the electronic assembly is made of two printed circuit boards (PCB) (diameter $\sim$ 40 mm, eight layers and 0.8 mm thickness) linked by a board to board connector. Both ASICs CINESIC32 and their external components are placed on one side of one PCB (at the bottom) while the other PCB (at the top) contains the MSP430 microcontroller, the wireless power module and the RF components.

The electronic boards are manufactured in accordance with ISO standard 13485. All manufactured PCBs undergo a production test phase where all functionalities are tested. In particular, during this phase each recording channel is individually characterized and a calibration file created in order to compensate the variations in gain and offset resulting from component dispersion. Moreover, in order to increase the reliability, all electronic

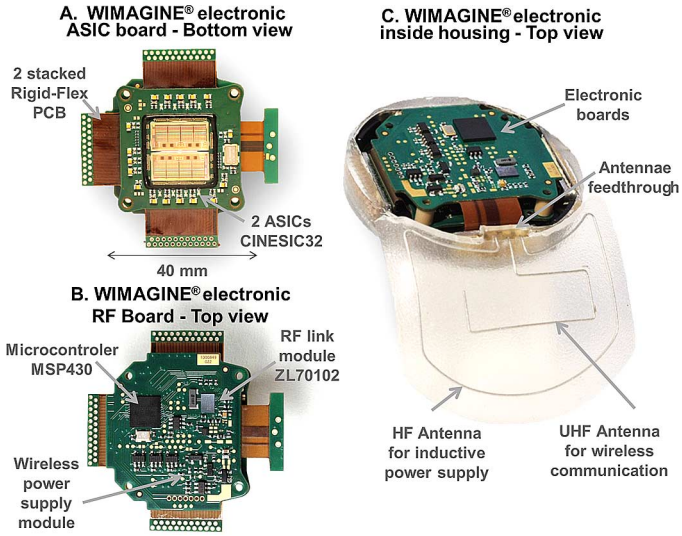

Fig. 7. Electronic boards of the implant.

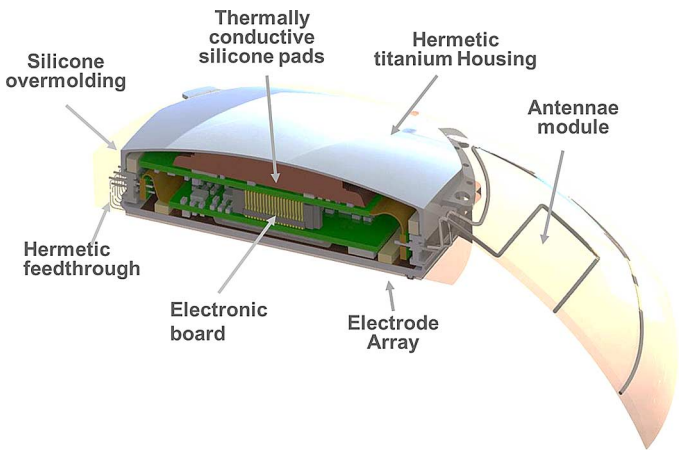

Fig. 8. Packaging of the implant.

boards undergo a burn-in procedure to avoid early in-use system failures.

Currently, several tens of manufactured PCBs were tested and burned. This procedure guarantees the reliability of the electronic boards which are integrated into an implant. Also, all functionalities (concerning the electrode array, the electronic board and the antennae module) of the manufactured implants are tested thanks to a specially designed test bench.

In addition, to complete the functional tests applied on each implant manufactured, a procedure dedicated to validate the performances of the global system was applied on the entire setup composed of two implants, base station and headset. Finally, in compliance with the IEC 62304, the firmware of the implant and the base station were tested at the unit, item and system level.

B. Implant Packaging

For safety requirements, it was decided to put all the electronics in a hermetic housing. Thus, a dedicated titanium packaging has been designed with dedicated hermetic feedthroughs. The latter are based on a ruby insulator and the hermeticity is achieved by gold brazing (Fig. 8). All these parts are individually tested in terms of helium leakage and yield 10^{-9} bar $\cdot$ cm^3 $\cdot$ s^{-1}. Once the PCBs are placed in the titanium housing by means of plastic fixing parts, both titanium parts are laser welded together and to the feedthroughs. Then the leakage level is tested again and the assemblies are accepted if the leakage level is below 10^{-8} bar $\cdot$ cm^3 $\cdot$ s^{-1}.

As any active implantable medical device (AIMD), our system consumes energy and produces heat that is transmitted to the surrounding tissues. The heat transfer must be controlled so that elevation of temperature is less than 2°C, according to the Directive 90/385/EEC [35].

In order to avoid any hot points, the thermal management is done by optimizing the PCB stacking using conductive glue and heat sinks. Moreover, thermally conductive silicone pads are placed between the top electronic boards and the titanium housing. The heat is homogenized and transmitted to the whole titanium surface (16 cm^2). As the overall power in the implant is lower than 350 mW (taking into account the inductive power transmission efficiency), the power density is approximately 22 mW/cm^2. Reference [36] reported a maximum limit at 80 mW/cm^2 for an AIMD, considering the appearance of necrosis in muscle tissue.

C. Electrode Array

The electrode array is composed of 64 recording electrodes, the active part of which is a 2-mm disk placed 0.15 mm below the silicone sheet, and three reference electrodes which are ten times the size of a recording electrode. The electrode array is mainly made of silicone rubber MED 4750 and platinum iridium 90/10. The silicone MED 4750 is a medical grade reference unrestricted in terms of implantation duration. The contacts are made of platinum iridium 90/10 connected to platinum iridium wires coated with polyurethane USP Class VI. The biocompatibility tests were made with a mock-up device consisting of a sandwich of materials reproducing the stack of materials and manufacturing processes. The scale was adapted to the chosen animal model as described in Section II-F.

D. Antennae

Two antennae have been designed for two separate links and are located outside the titanium housing: one antenna for HF inductive powering and the other for UHF communication.

1) HF Antenna: The HF antenna is designed to provide up to 30 mA at 3.3 V and is associated with an RF front-end embedded on the electronic board, including a rectifying stage, a shunt regulator and ultra-low noise LDOs (low-dropout linear regulator). Its area is 10 cm^2. The HF implant antenna and the HF generator antenna were dimensioned together for optimizing the transmitted power for a nominal distance of 25 mm between both antennas.

2) UHF Antenna: The UHF antenna is connected to the electronic board through a SAW filter to prevent interference from strong out-of-band RF signals. The gain of the implantable antenna has been measured to -29 dBi and throughput tests have been performed by placing the packaged implant with its platinum antenna in a human head phantom (Fig. 9).

An effective data throughput of 450 kb/s between the implant and the base station was measured over several hours at a distance of 2 m. These tests confirmed the feasibility of

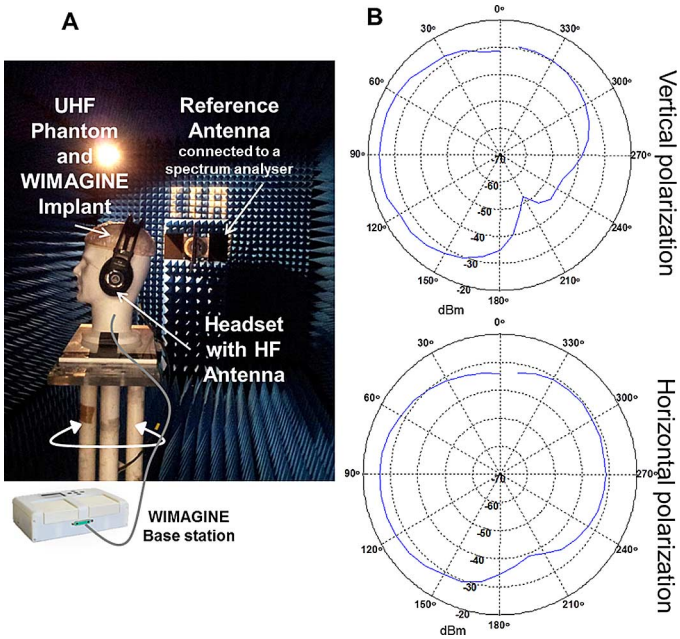

Fig. 9. (A) Anechoic chamber set up for radiation pattern measurement of implant's UHF antenna and (B) radiation pattern of the designed implantable antenna: measured antenna gain −29 dBi.

transmitting 32 channels with a 12-bit resolution sampled at ∼ 1 kHz per channel.

3) Implant Antennae Module: These two HF and UHF antennae are inserted one into the other, in order to optimize the surface of the external implant antenna module, and are designed and optimized to perform simultaneously. Moreover, these two combined antennae are made with two platinum wires embedded in a liquid silicone elastomer, in order to respect the rules of biocompatibility.

E. WIMAGINE Platform

The WIMAGINE platform is made up of two WIMAGINE implants, a base station and a PC application.

1) HF Headset: In order to position and maintain the remote HF power supply antennae in front of the implanted antennae, an audio headset was modified to release the patient's auricular pinnae. The helmet hoop contains two antennae to provide HF power supply to the two implants (Fig. 10). A helmet-positioning aid is displayed on the user interface software, to help positioning the HF antennae in front of the implant antenna.

2) Base Station: A base station has been designed to act as a gateway between the PC application and up to two implantable devices. It provides the inductive link for powering each implant, the means for establishing a communication with each implant in the MICS band and can be connected to a PC through Ethernet or USB. It also includes isolated analog and digital inputs and outputs that can be used for instance for synchronous BCI protocols (Fig. 10). The whole base station is packaged into a compact 24 cm × 16 cm × 6.5 cm housing.

3) PC Application: A PC application has been designed for interfacing the implants and the base station through the high level communication protocol. It is able to record the signals in a standard SMR format and can stream all the data in real

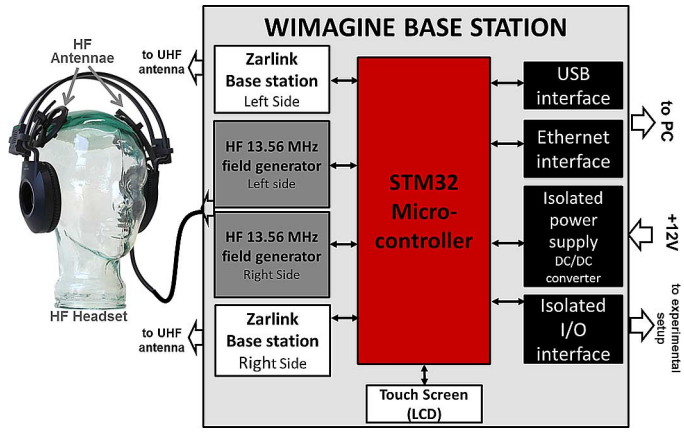

Fig. 10. Helmet providing remote power supply and Base station block diagram.

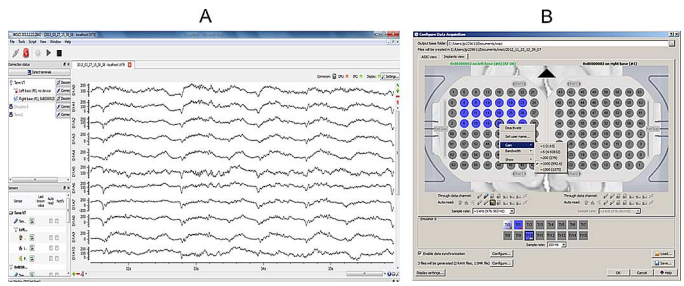

Fig. 11. PC user interface. A: ECoG display; B: Choice of recording electrodes on both implants.

time to a "Fieldtrip" network buffer. It synchronizes and displays data streams including the implants' ECoG signals and the base station's input triggers according to the user's request. Moreover, it controls the power supply of each implant, relays the configuration commands specified in a graphical view by the user (Fig. 11), reads the different sensor values, and gives access to debug and maintenance features (ping and throughput tests, real-time protocol control and debug). The PC application has been optimized to reduce the propagation delay of the signals: it takes less than 5 ms for a signal to be relayed from the electrodes to the PC platform. This delay may be increased by 30 to 100 ms depending on the radio communication link quality.

F. In Vivo Evaluations

1) ½ Scale Devices for Nonhuman Primate Implantation: In order to perform *in vivo* evaluations (implantation test and electrical impedance spectroscopy) in nonhuman primates, a half-scale device was designed integrating all materials of the device without the electronic components. This assembly consists of a cylinder of T40 titanium according to the ASTM F67 (25 mm in diameter and 2 mm in height) on which is glued (by means of a silicone adhesive, Silicone Nusil MED2-4213) the electrode array (Statice Santé company, BCI primate model, Platinum-iridium electrodes and silicone Nusil MED-4750). A molding is then made by means of the silicone Nusil MED-6210 and the interface between the silicone MED-6210 and the titanium is optimized by means of the adhesion promoter MED1-161. For

test on nonhuman primates, decontamination and Tyvek bagging were performed in a CEA/LETI cleanroom. The devices were cleaned and then sterilized with ethylene oxide.

Note that for implantation in monkey 2 (biocompatibility evaluation and Electrical Spectroscopy Impedance), the device was connected to the experimental setup using an Amphenol PL900 connector hosted in a peek box that protects the connector from moisture or dust. This implantation also investigates if the curvature mismatch between the flat WIMAGINE implant and the curved surface of the brain will be an issue. MRI measurements estimated a curvature mismatch of 1.3 mm for the half sized device on the nonhuman primate.

2) Animals and Surgical Procedure: Experiments were conducted on two cynomolgus monkeys: monkey 1 (Macaca Mulatta, Bioprim, Baziege): age 14 years old, weight 14 kg, and monkey 2 (Macaca Mulatta, Silabe, Strasbourg): 4 years old and 8.6 kg. All experiments were carried out in accordance with the recommendations of the European Community Council Directives of 1986 (86/609/EEC) and the National Institutes of Health Guide for the Care and Use of Laboratory Animals. The Ethics Committee COMETH approved the experimental protocol. Animals were kept with other congeners in an air-conditioned room under standard conditions of temperature ($23 \pm 1^{\circ}$C), humidity ($65\% \pm 4\%$), light (12 h light/dark cycle), and food/water available ad libitum. Monkeys were monitored clinically and their motricity was evaluated periodically with a motion tracking system. We did not observe motor deficits along the living period.

After induction under general anesthesia with ketamine–xylazine (10mg–1mg/kg, im, Imalgene, Centravet, France), the monkey's head was fixed in a Kopf stereotaxic frame (David Kopf Instruments, Tujunga, CA, USA). All operations were performed under sterile conditions. For both monkeys, 25 mm-diameter craniotomies were performed with a trephine to place the ½ scale device.

3) Tissue Preparation and Histological Analysis of Brain Reactivity: Twenty-six weeks after implantation, the monkey 1 was perfused transcardially with 0.9% NaCl followed by 10% formaline. In order to avoid damaging the brain tissue during histological procedures, the monkey brain including the device and the skull were fixed in 4% formaline. After fixation, the device was carefully removed to test the adhesion to dura mater and bone. The brain was then removed and postfixed overnight in the same fixative. Next, the brain was placed in phosphate-buffered saline (PBS) with the addition of 30% sucrose until the block sank. Before freezing, the brain was cut to form a block and both tissues covered with the implant and the control tissues were investigated. The brain was then sectioned coronally and serially (at 50 μm) using a freezing microtome. Sections were collected and were processed for Nissl staining and immunohistochemistries for glial fibrillary acidic protein (GFAP) and ionized calcium-binding adapt molecule 1 (Iba1). Sections were incubated with the following primary antibody solutions overnight at 4°C including: GFAP (1:500, polyclonal rabbit IgG, Dakocytomation, Glostrup, Denmark) to identify astrocytes, Iba1 (1/1000, polyclonal rabbit IgG, Wako Chemicals GmbH, Neuss, Germany) to identify macrophage/microglia. Secondary antibodies were diluted 1:1000 and included goat anti-rabbit IgG Alexa 488 (Molecular Probes) for GFAP and Iba1. All sections were counterstained by incubation with the nuclear dye Propidium Iodide (PI, Sigma). Sections treated only with secondary antibody but with no primary antibody were used to determine nonspecific binding. Tissue sections were mounted with Fluorsave (Merck KGaA, Darmstadt, Germany) and bound primary antibodies were visualized on a confocal microscope (Olympus, Hamburg, Germany).

III. Results

A. Design Validation

1) Functional Test: The functionality of several fully assembled implants has been evaluated using an automated test bench. The implant was powered remotely using the designed inductive link supplied by the base station and communication was established with a PC using the MICS band. In order to perform an evaluation of the noise of the overall system, the reference electrodes were shorted with the measuring electrodes, revealing an overall input referred noise of 1 μV_{RMS} in the 0.5–300 Hz band on each electrode of the fully assembled implant.

2) Packaging Hermeticity Validation: The electronic is sealed in a hermetic titanium housing and the electrode array and the antennae are connected to the hermetic feedthroughs. The hermeticity level was measured using helium leakage tests according to the NF EN 60068-2-17 standard. The maximum leakage rate measured on the first series is $3*10^{-9}$ bar$\cdot$cm$^3\cdot$s^{-1} for a threshold set at 10^{-8} bar $\cdot$ cm^3 $\cdot$ s^{-1}. The packaging satisfies the requirements and is in accordance with a long term implantation.

3) Heating Evaluation: This risk of heating tissue is still under assessment, nevertheless early results were obtained with the implant immerged in water and powered remotely. The total power cannot be assessed by simulation since there would be a major approximation in the yield of the inductive link. Consequently, the total power was measured using a differential calorimeter. The reference chamber hosts a controlled dissipative system and the second chamber hosts the implant wirelessly powered by the inductive link. In steady state we can deduce the total power dissipation of the system. A measured maximum value of 350 mW was obtained, which includes the loss in the platinum antenna and in the rectifying stage.

The implant is equipped with thermocouples on its titanium surface but also in the housing, on the PCB close to the hot point and on the electrode array. The hot points are reduced thanks to a stack of gap pad and gap filler coupled by with a copper sheet and pyrolytic graphite. The temperature is made homogeneous and then mainly transferred to the skin which is considered less sensitive than the brain.

On the titanium surface the temperature is measured by five thermal probes on a diagonal that crosses the hot spot of the PCB underneath. The implant was immerged into a water tank and switched on until a steady state was reached. The maximum temperature is obtained on the titanium surface; it reaches temperatures in the range of 1.0°C above the water temperature whereas on the electrode array it reaches 0.3°C. Note that thanks to the assembly of conductive silicone and heat sinks located inside the housing, the temperature heterogeneity on the titanium

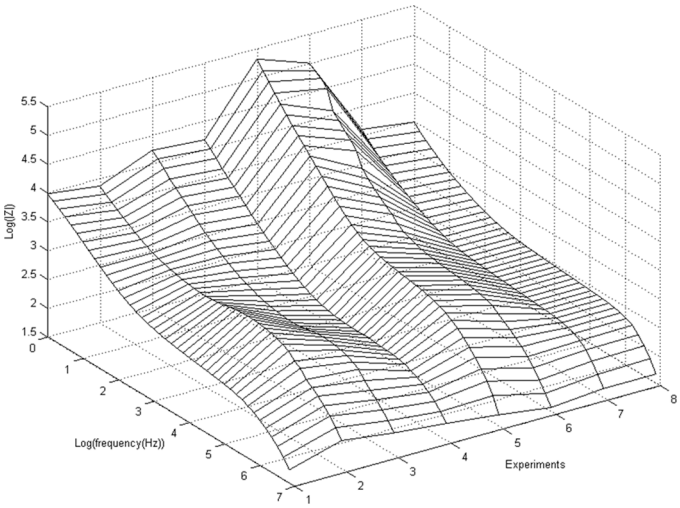

Fig. 12. One year follow up of the mean impedance of the cortical grid.

surface was limited to 0.2°C. WIMAGINE is also tested with respect to EN 45502-1 standard by external certified laboratories. Prequalification tests show an increase of temperature of less than 1°C. Regarding long term effects, simulations have been performed and implantation on large animals are scheduled.

B. In Vivo Evaluations

1) In Vivo Impedance Evaluation of Electrode Array: The knowledge of the impedance and its evolution along time is an important parameter to design the analog front end, the signal processing and to check the tolerance of the electrodes using a functional criterion. A cortical grid reduced to 25 mm as described for the biocompatibility study was implanted extradurally but for the impedance monitoring the grid is connected to an Amphenol Connector (PL900) by the means of biocompatible wires. The connector is placed in a watertight packaging made of PEEK.

In Fig. 12 we plotted the logarithm of the impedance modulus (X axis) with respect to the logarithm of the frequency (Y axis) for several sessions. Despite the variability of the results, Fig. 12 shows that the impedance is low just after the implantation, then increases as the edema disappears and eventually converges to an intermediate value confirming the local tolerance of the grid. Eight experiments are plotted corresponding to eight sessions during the one year of recording. This is also in accordance with [37].

2) In Vivo Recording Evaluation: In order to validate the functionalities of the WIMAGINE platform, *in vivo* validation tests were performed. The goal was to record the ECoG of a nonhuman primate implanted with a silicone-platinum cortical electrode array. As the size of the WIMAGINE implant is too large to be implanted on a nonhuman primate, the WIMAGINE implant has been connected to the implanted ECoG electrode array through a transcutaneous connector. The nonhuman primate was stimulated by the means of a Micromed Energy Light peripheral nerve stimulator at the right anterior limb in order to record somatosensory evoked potentials (SEP). The trigger signal corresponding to the stimulation event was recorded using the base station and synchronized with the neural signals (Fig. 13). The

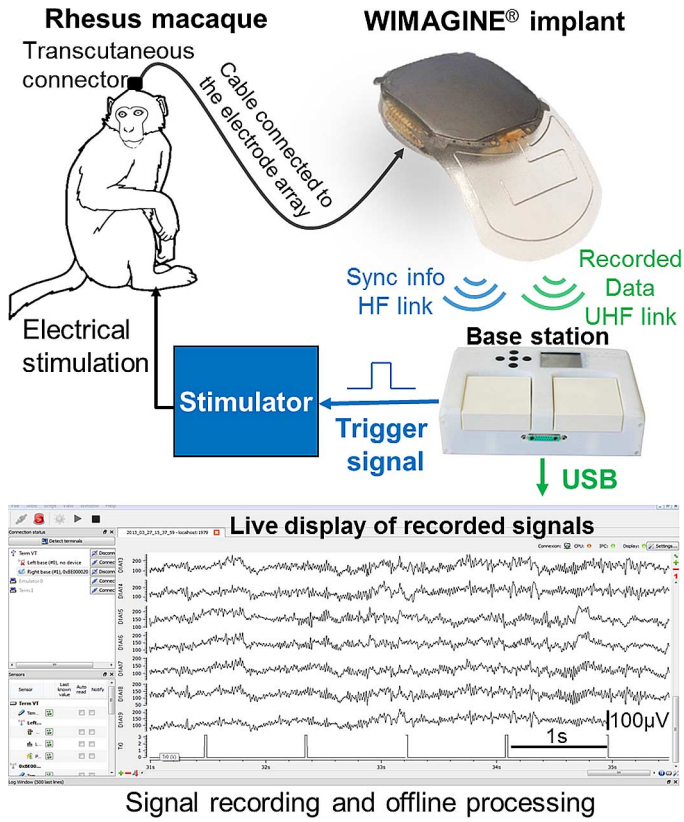

Fig. 13. Experimental setup for SEP acquisition.

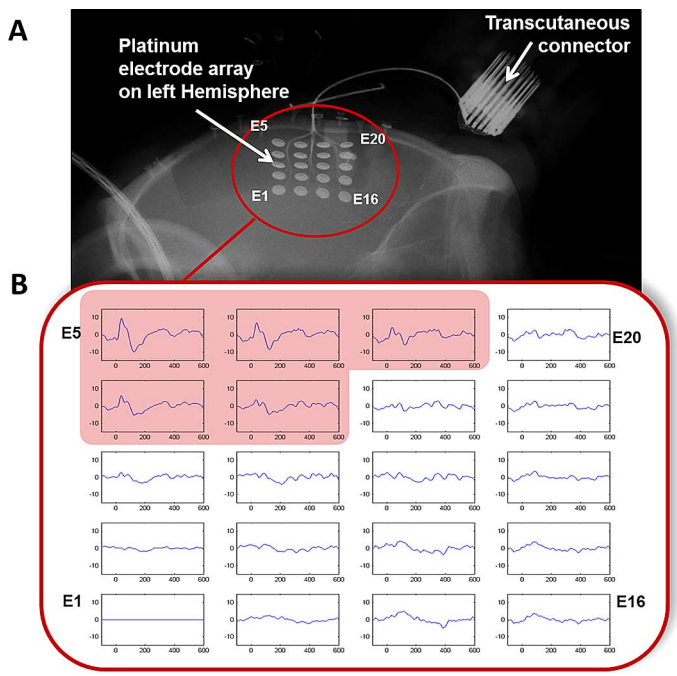

Fig. 14. (A) Localization of the implanted ECoG recording electrode array on the left hemisphere. (B) Extracted SEP for each electrode according to electrode placement of "A". Shaded electrodes correspond to electrodes 4, 5, 9, 10 and 15 which are placed over the somatosensory area. X axis: ms, Y axis:μV.

epochs corresponding to 535 stimuli were averaged and band pass filtered (1 Hz – 30 Hz). As shown in Fig. 14, the response is mainly localized on the electrodes placed in the area corresponding to the right leg.

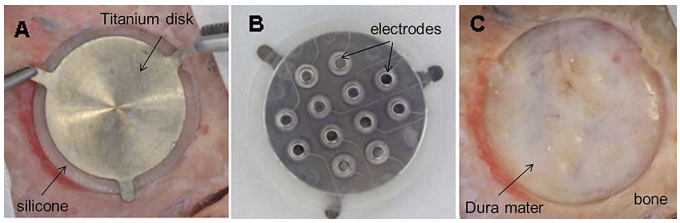

Fig. 15. Implanted 1/2 scale device on the dura mater in monkey 1: (A) After 26 weeks. (B) Explanted device after 26 weeks. (C) Dura mater in contact with the device after 26 weeks.

Two healthy Macaca Rhesus have been implanted with an electrode array in the epidural or in the subdural space for long term ECoG recording, one for 11 months, and the second one for 8 months. Ten Sensory Evoked Potentials experiments have been performed for the first monkey, six for the second. No degradation of the signal quality was observed in either case.

C. Long Term Biocompatibility Evaluation

Histological examinations were carried out post-mortem, 26 weeks after implantation, for monkey 1. After euthanasia of the animal and removing skin and muscles covering the implants, observation of the implantation sites showed no encapsulation of the implants after 26 weeks (Fig. 15).

The adhesion of the electrode array and the MED-6210 over-molding silicone with tissue in contact (dura mater beneath the implant, dura mater's substitute and skull bone at the periphery) was also tested. The implants were freely removed without damaging the dura mater or the substitutive tissue and no macroscopic sign of tissue defect was observed for the epidural (Fig. 15) and the subdural (data not shown) locations. Immediately after explantation, devices were inspected and observed under a stereomicroscope. There was no sign of degradation or dissociation (data not shown). After removal of the skull, brain tissues were prepared for microscopic examination in order to evaluate tissue reaction in contact with the implant (dura mater, brain cortex and leptomeninges structures) and at distance (glia limitans and brain cortex).

As shown in Fig. 16, observations of the dura mater and the leptomeninges covered by the epidural implant revealed no histopathological changes. The thickness of the implant-covered dura mater was compared to the implant-uncovered dura mater. The thickness of the first one is 98.8 ± 2.4 μm and 99.3 ± 3.4 μm for the control. The subdural implant induced the development of a tissue that substitutes the dura mater after a 26 weeks contact duration. We showed that the thickness of this tissue did not differ significantly from the constitutive dura mater. The second part of histological investigations was conducted to evaluate brain cortex reaction beneath the epidural implant and to detect signs of inflammation. The reactive gliosis is the endogenous response of brain tissue to aggression and corresponds to the accumulation and/or recruitment of glial cells (astrocytes and microglia). The glial activation is the release of glial factors that will act on target cells in the same way than the cellular immune response and thus promote peripheral monocyte infiltration (especially macrophages and lymphocytes). Immunohistochemical studies were performed for detecting signs

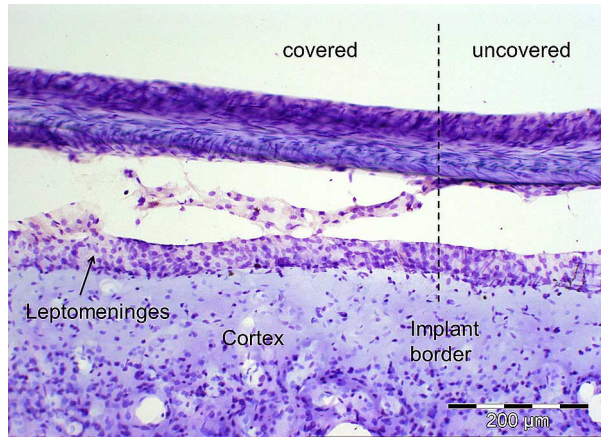

Fig. 16. Histological slice demonstrating the absence of tissue reaction after 26 weeks. Covered and uncovered parts of the brain tissue with dura-mater, leptomeninges and brain cortex (Nissl staining).

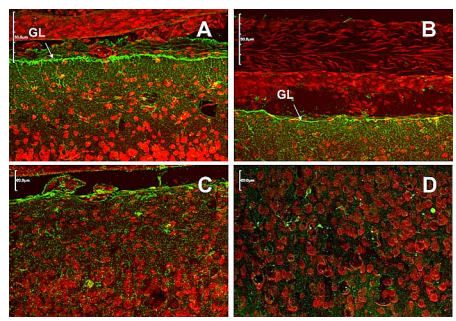

Fig. 17. Representative glial fibrillary acidic protein (GFAP) expression patterns in (A) epidural implant-covered brain cortex and (B) in epidural implant-uncovered brain cortex. Scale bar $= 50$ μm. Representative ion calcium binding adaptor molecule 1 (Iba1) expression pattern in (C) epidural implant-covered brain cortex and (D) epidural implant-uncovered brain cortex. Scale bar $= 20$ μm. GL: glia limitans.

of reactive gliosis and monocyte infiltration in the brain cortex. The results are shown in Fig. 17.

Representative patterns of cortical GFAP expression in implant-covered and implant-uncovered brain cortex areas are shown in Fig. 17(a) and (b). Note that expression of the astrocyte marker is highly concentrated in the glia limitans. In implant-covered brain cortex, there was no loss of continuity for the glia limitans and reactive astrocytes in the cortex. These findings reveal that the epidural implant does not damage the GL and does not induce astrogliosis into the cortex under the implant.

Representative patterns of cortical Iba1 expression in implant-covered and implant-uncovered brain cortex areas are shown in Fig. 17(c) and (d). Immunostaining raised against the protein Iba-1 (ionized calcium-binding adapt molecule 1 expressed by microglia and macrophages) showed the absence of activated microglial cells into the brain cortex beneath the implanted device after 26 weeks. These results suggest that the epidural implant does not induce inflammation after a 26 weeks period.

IV. Discussion

The WIMAGINE implant has been designed to fulfill the requirements of a fully implantable device for recording ECoG

TABLE II
STATE-OF-THE-ART OF NEURAL RECORDING IMPLANTABLE

	Borton[25]	**Rizk [38]**	**Harrison [39]**	**Schuettler [26]**	**Hirita [27]**	**This work**
Type	Spikes	Spikes	Spikes	ECoG	ECoG	**ECoG**
Sampling Frequency	20 kHz	31.25 kHz	15,7 kHz	1 kHz	1kHz	**1 kHz**
Number of channels	100	96	100	16	128	**64**
Bandwidth	0.1Hz - 7.8kHz	n.r.(not reported)	250Hz - 5kHz	0.1Hz - 500Hz	0.1Hz - 1000Hz	**0.5Hz - 300Hz**
Resolution	12bit (LTC2366)	12bit	10bit	16 bit	12 bit	**12bit**
Input referred noise	8.6µVRMS	n.r.	30-40 µVRMS	n.r.	2.8 µV (0.1 - 100Hz)	**1µV_{RMS} [0.5Hz - 300Hz]**
Power consumption	In use: 90.6 mW In charge: 430 mW	2000 mW	8 mW	n.r.	Wireless Data: 300mW - Wireless Supply: 4W	**75mW (32ch @ 1kHz)**
Wireless Data rate	24 Mbps	n.r.	345,6 kbps	1 Mbps	400 kbps (128ch x 12bit)	**450 kbps**
Wireless Data transfer type	RF: 3.2 - 3.8 GHz IR: 850nm	916.5 MHz	902-928 MHz FSK	IR: 880nm - 900nm	2.45 GHz	**MICS band 402-405 MHz**
Size	56x42x11 mm	n.r.	Utah Array flip-chip	78x34x5 mm	20x30x2.5 mm & 60x60x8 mm	**50mm diameter Antenna : 10cm²**

signals for long term clinical applications. The constraints of an implantable active medical device (AIMD) such as ultra-low power, miniaturization, safety, reliability and compliance with applicable regulations (EN 45502-1) have been addressed during the design phase. The designed implant has been validated functionally, the heating of the device has been assessed and biocompatibility studies and *in vivo* recordings have been performed.

The *in vivo* recorded SEP shoved the feasibility of recording neurological signals with high accuracy using the designed ASIC and the platinum electrode array while powering the implant remotely. The implant excels particularly in recording very low amplitude signals with extremely low input referred noise. The overall performances of the designed implant are compared to state-of-the art work in neural recording devices in Table II.

The biological evaluation of any material or medical device for use on humans must be part of a structured biological evaluation within a risk management process in accordance with ISO 14971. The long-term biocompatibility is evaluated according to the parts 6 and 11 of the ISO 10993 norm consisting of the study of local and systemic effects respectively after a 26 weeks contact duration in animal. The ISO 10993 recommends association of these two parts in a same protocol to reduce the number of animals. For this evaluation, we have produced cylindrical sticks from the four materials in contact with the living tissue and have implanted them subcutaneously. After a 26 weeks period, local tolerance and systemic toxicity will be evaluated with histological approach by a certified laboratory.

A passive device was developed and implanted epidurally or subdurally on nonhuman primates for 26 weeks six months. These *in vivo* trials have enabled us to investigate surgical implantation techniques and to demonstrate benefits of epidural (extra-dural) implantation of the device. The end-stage healing response to biomaterials is generally fibrous encapsulation. In the current study, the device implanted on nonhuman primate dura mater was found to be neither reactive nor encapsulated. An explanation for the absence of fibrous encapsulation may be due to the fact that the dura mater was not injured and meningeal fibroblasts were not activated. The absence of fibrotic scar tissue was confirmed by microscopic examination and there was no thickening of dura mater in contact with the device. The subdural implantation of the device induced the development of a biological tissue which acts as a dura mater and with a similar thickness. These data clearly suggest that the benefit obtained from ECoG signals with subdural implants could be lost in long term implantation.

After euthanasia of the animal and fixative intracardiac perfusion, the devices were carefully and manually removed from the implantation site and there was no focal adhesion between materials and living tissue but only imprints of electrodes. This data suggest that epidural or subdural devices can be easily explanted by the neurosurgeon. This data suggests that EcoG recording may be operational in the long term, ensuring the functionality of the BCI. Finally, the fact that the body reacts and induces the formation of a substitutive biological tissue under the subdurally implanted device and the fact that it has not been reported that subdural implantation would provide better signal quality in the long term having driven the choice of epidural implantation.

However, some additional tests remain to be done in order to fully validate the conformance with the applicable regulations and standards. In particular, aspects regarding the thermal dissipation of the implant will be further investigated. As shown in the result section, the thermal management of the implant was optimized using passive components to avoid hot spots and to minimize the overall temperature of the implant in water. The temperature increase is in the range of 1.0°C which is below the requirement of the EN 45502-1. To extrapolate this result to the thermal behavior of the implant *in vivo*, the bio-thermal effects shall be taken into account and implemented in a numerical model.

The next steps include also the manufacturing according to a qualified industrial process under ISO certification 13485.

There are various possible applications using the WIMAGINE implant. The main application currently developed at Clinatec is a BCI platform to allow a quadriplegic subject to recover some mobility using effectors such as a four-limb exoskeleton. Movements imagined by the subject induce in his motor cortex electrical activity which is recorded by the implants and processed in real time by the BCI software platform, to control effectors after a training period.

The BCI software platform has been designed and tested through preclinical studies on rats and nonhuman primates [28], [40], [41].

The WIMAGINE implant can also be used for ECoG recording for shorter periods of time in order to monitor the electrical activity of the brain as a presurgical evaluation tool for seizure detection. The fact that the device is wireless allows use of it like a "Holter" device during normal daily activities. Future developments include a stimulation capacity for various applications such as closed loop systems for seizure, pain or severe resistant depression.

ACKNOWLEDGMENT

The authors wish to thank CEA/LETI DTBS, DSIS and DACLE teams for their profound involvement in the implant design, and the CLINATEC team for preclinical and histology studies, as well as integration, optimization and test of the implant.

REFERENCES

[1] S. Silvoni, A. Ramos-Murguialday, M. Cavinato, C. Volpato, G. Cisotto, A. Turolla, F. Piccione, and N. Birbaumer, "Brain-computer interface in stroke: A review of progress," *Clin. EEG Neurosci.*, vol. 42, no. 4, pp. 245–52, Oct. 2011.

[2] C. Mehring, M. P. Nawrot, S. C. de Oliveira, E. Vaadia, A. Schulze-Bonhage, A. Aertsen, and T. Ball, "Comparing information about arm movement direction in single channels of local and epicortical field potentials from monkey and human motor cortex," *J. Physiol. Paris*, vol. 98, pp. 498–506, 2004.

[3] E. C. Leuthardt, G. Schalk, J. R. Wolpaw, J. G. Ojemann, and D. W. Moran, "A brain-computer intefrace using ElectroCorticoGraphic signals in humans," *J. Neural Eng.*, no. 1, pp. 63–71, 2004.

[4] E. C. Leuthardt, K. J. Miller, G. Schalk, R. P. Rao, and J. G. Ojemann, "Electrocorticography-based brain computer interface—The Seattle experience," *IEEE Trans. Neural Syst. Rehabil. Eng.*, vol. 14, no. 2, pp. 194–198, Mar. 2006.

[5] G. Schalk, J. Kubánek, K. J. Miller, N. R. Anderson, E. C. Leuthardt, J. G. Ojemann, D. Limbrick, D. Moran, L. A. Gerhardt, and J. R. Wolpaw, "Decoding two-dimensional movement trajectories using ElectroCorticoGraphic signals in humans," *J. Neural. Eng.*, vol. 4, pp. 264–275, 2007.

[6] R. Scherer, B. Graimann, J. E. Huggins, S. P. Levine, and G. Pfurtscheller, "Frequency component selection for an ECoG-based brain-computer interface," *Biomed. Tech. (Berl)*, vol. 48, pp. 31–36, 2003.

[7] E. A. Felton, J. A. Wilson, J. C. Williams, and P. C. Garell, "Electrocorticographically controlled brain-computer interfaces using motor and sensory imagery in patients with temporary subdural electrode implants. Report of four cases," *J. Neurosurg.*, vol. 106, pp. 495–500, 2006.

[8] A. G. Rouse and D. W. Moran, "Neural adaptation of epidural electrocorticographic (EECoG) signals during closed-loop brain computer interface (BCI) tasks," in *Proc. IEEE EMBS 2009*, pp. 5514–5517.

[9] W. Wang, S. S. Chan, D. A. Heldman, and D. W. Moran, "Motor cortical representation of position and velocity during reaching," *J. Neurophysiol.*, vol. 97, no. 6, pp. 4258–4270, 2007.

[10] T. Pistohl, T. Ball, A. Schulze-Bonhage, A. Aertsen, and C. Mehring, "Prediction of arm movement trajectories from ECoG-recordings in humans," *J. Neurosci. Methods*, vol. 167, no. 1, pp. 105–114, 2008.

[11] J. C. Sanchez, A. Gunduz, P. R. Carney, and J. C. Principe, "Extraction and localization of mesoscopic motor control signals for human ECoG neuroprosthetics," *J. Neurosci. Methods*, vol. 167, pp. 63–81, 2008.

[12] J. Kubanek, K. J. Miller, J. G. Ojemann, J. R. Wolpaw, and G. Schalk, "Decoding flexion of individual fingers using ElectroCorticoGraphic signals in humans," *J. Neural Eng.*, vol. 6, no. 6, p. 066001, 2009.

[13] G. Schalk, K. J. Miller, N. R. Anderson, J. A. Wilson, M. D. Smyth, J. G. Ojemann, D. W. Moran, J. R. Wolpaw, and E. C. Leuthardt, "Two-dimensional movement control using ElectroCorticoGraphic signals in humans," *J. Neural Eng.*, vol. 5, pp. 75–84, 2008.

[14] A. P. Georgopoulos, J. F. Kalaska, R. Caminiti, and J. T. Massey, "On the relations between the direction of two-dimensional arm movements and cell discharge in primate motor cortex," *J. Neurosci.*, vol. 2, no. 11, pp. 1527–1537, Nov. 1982.

[15] A. B. Schwartz, R. E. Kettner, and A. P. Georgopoulos, "Primate motor cortex and free arm movements to visual targets in three-dimensional space. I. Relations between single cell discharge and direction of movement," *J. Neurosci.*, vol. 8, no. 8, pp. 2913–2927, Aug. 1988.

[16] D. W. Moran and A. B. Schwartz, "Motor cortical representation of speed and direction during reaching," *J. Neurophysiol.*, vol. 82, no. 5, pp. 2676–2692, Nov. 1999.

[17] W. Wang, S. S. Chan, D. A. Heldman, and D. W. D. W. Moran, "Motor cortical representation of hand translation and rotation during reaching," *J. Neurosci.*, vol. 30, no. 3, pp. 958–962, 2010.

[18] M. D. Serruya, N. G. Hatsopoulos, L. Paninski, M. R. Fellows, and J. P. Donoghue, "Instant neural control of a movement signal," *Nature*, vol. 416, no. 6877, pp. 141–142, 2002.

[19] D. M. Taylor, S. I. Tillery, and A. B. Schwartz, "Direct cortical control of 3D neuroprosthetic devices," *Science*, vol. 296, no. 5574, pp. 1829–1832, 2002.

[20] M. Velliste, S. Perel, M. C. Spalding, A. S. Whitford, and A. B. Schwartz, "Cortical control of a prosthetic arm for self-feeding," *Nature*, vol. 453, no. 7198, pp. 1098–1101, Jun. 2008.

[21] L. R. Hochberg, M. D. Serruya, G. M. Friehs, J. A. Mukand, M. Saleh, A. H. Caplan, A. Branner, D. Chen, R. D. Penn, and J. P. Donoghue, "Neuronal ensemble control of prosthetic devices by a human with tetraplegia," *Nature*, vol. 442, no. 13, pp. 164–171, 2006.

[22] P. J. Rousche and R. A. Normann, "Chronic recording capability of the Utah intracortical electrode array in cat sensory cortex," *J. Neurosci. Methods*, vol. 82, pp. 1–15, 1998.

[23] X. Liu, D. B. McCreery, R. R. Carter, L. A. Bullara, T. G. Yuen, and W. F. Agnew, "Stability of the interface between neural tissue and chronically implanted intracortical microelectrodes," *IEEE Trans. Rehabil. Eng.*, vol. 7, no. 3, pp. 315–326, May 1999.

[24] S. Suner, M. R. Fellows, C. Vargas-Irwin, G. K. Nakata, and J. Donoghue, "Reliability of signals from a chronically implanted, silicon-based electrode array in non-human primate primary motor cortex," *IEEE Trans. Neural Syst. Rehabil. Eng.*, vol. 13, no. 4, Dec. 2005.

[25] D. A. Borton, M. Yin, J. Aceros, and A. Nurmikko, "An implantable wireless neural interface for recording cortical circuit dynamics in moving primates," *J. Neural Eng.*, vol. 10, p. 026010, 2013.

[26] M. Schuettler, F. Kohler, J. S. Ordonez, and T. Stieglitz, "Hermetic electronic packaging of an implantable brain-machine-interface with transcutaneous optical data communication," in *Conf. Proc. IEEE Eng. Med. Biol. Soc.*, Aug. 2012, vol. 2012, pp. 3886–3889.

[27] M. Hirata, K. Matsushita, T. Suzuki, T. Yoshida, S. Morris, T. Yanagisawa, and T. Yoshimine, "A fully-implantable wireless system for human brain-machine interfaces using brain surface electrodes: W-HERBS," *IEICE Trans. Commun.*, vol. 94, no. 9, pp. 2448–2453, 2011.

[28] A. Eliseyev, C. Moro, J. Faber, A. Wyss, N. Torres, C. Mestais, A. L. Benabid, and T. Aksenova, "L1-Penalized N-way PLS for subset of electrodes selection in BCI experiments," *J. Neural Eng.*, vol. 9, p. 045010, 2012.

[29] T. Pistohl, A. Schulze-Bonhage, A. Aertsen, C. Mehring, and T. Ball, "Decoding natural grasp types from human ECoG," *NeuroImage*, vol. 59, pp. 248–260, 2012.

[30] S. Robinet, P. Audebert, G. Régis, B. Zongo, J. F. Bêche, C. Condemine, S. Filipe, and G. Charvet, "A low-power 0.7 VRMS 32-channel mixed-signal circuit for ECOG recordings," *IEEE J. Emerging Sel. Topics Circuits Syst.*, vol. 1, no. 4, pp. 451–460, Dec. 2011.

[31] M. Foerster, J. Porcherot, S. Bonnet, A. Van Langhenhove, S. Robinet, and G. Charvet, "Integration of a state of the art ECoG recording ASIC into a fully implantable electronic environment," in *Proc. Biomed. Circuits Syst. Conf.*, Nov. 28–30, 2012, p. 232,235.

[32] *European Standard*, BS EN 45502–1, Feb. 1998, Active Implantable Medical Devices.

[33] ZL70101 MICS Transceiver Zarlink Semiconductor, 2011 [Online]. Available: http://www.zarlink.com

[34] M. Foerster, S. Bonnet, A. Van Langhenhove, J. Porcherot, and G. Charvet, "A synchronization method for wireless acquisition systems, application to brain computer interfaces," *Proc. IEEE EMBC Conf.*, 2013.
[35] *Directive 90/385/EEC*, [Online]. Available: http://eur-lex.europa.eu/LexUriServ/LexUriServ.do?uri=CONSLEG:1990L0385:20071011:fr:PDF
[36] T. M. Seese, H. Harasaki, G. M. Saidel, and C. R. Davies, "Characterization of tissue morphology, angiogenesis, and temperature in the adaptive response of muscle tissue to chronic heating," *Lab. Invest.*, vol. 78, pp. 1553–62, 1998.
[37] M. A. Thil, D. T. Duy, I. M. Colin, and J. Delbeke, "Time course of tissue remodelling and electrophysiology in the rat sciatic nerve after spiral cuff electrode implantation," *J. Neuroimmunol.*, vol. 185, pp. 1103–1103, 2007.
[38] M. Rizk, C. A. Bossetti, T. A. Jochum, S. H. Callender, M. A. Nicolelis, D. A. Turner, and P. D. Wolf, "A fully implantable 96-channel neural data acquisition system," *J. Neural Eng.*, vol. 6, no. 2, p. 026002, 2009.
[39] R. R. Harrison, R. J. Kier, C. A. Chestek, V. Gilja, P. Nuyujukian, S. Ryu, and K. V. Shenoy, "Wireless neural recording with single low-power integrated circuit," *IEEE Trans. Neural Syst. Rehabil. Eng.*, vol. 17, no. 4, pp. 322–329, Jul. 2009.
[40] A. Eliseyev, C. Moro, T. Costecalde, N. Torres, S. Gharbi, C. Mestais, A. L. Benabid, and T. Aksenova, "Iterative $\mathbb{N}$-way partial least squares for a binary self-paced brain-computer interface in freely moving animals," *J. Neural Eng.*, vol. 8, no. 4, p. 046012, Aug. 2011.
[41] A. Eliseyev and T. Aksenova, "Recursive $\mathbb{N}$-way partial least squares for brain-computer interface," *PloS One*, vol. 8, no. 7, p. e69962, 2013.

Corinne S. Mestais received the B.S. degree in electrical engineering from Institut National Polytechnique, Grenoble, France, in 1978, the M.Eng. degree in electrical engineering in 1979 from Cornell University, Ithaca, NY, USA, and the DESS degree in clinical psychology and psychopathology in 1993 from University Pierre Mendes-France, Grenoble.

She was a member of the Scientific Committee ANR-TECSAN for the French Ministry of Research from 2000 to 2010. Since 2008, she has been coordinating the Brain Computer Interface project under Prof. Alim-Louis Benabid's scientific direction at CEA-LETI-CLINATEC, Grenoble, France. Her main research interests concern the development of micronanotechnologies for health applications, especially in the field of handicap and neurodegenerative diseases. Since 2009, she has been an international expert at CEA in the field of medical instrumentation and microtechnologies for healthcare.

Guillaume Charvet received the B.S. degree in electrical engineering from Institut National Polytechnique, Grenoble, France, in 2001.

In 2002, he joined the CEA-LETI and he was in charge of the electronic design for an innovative DNA biochip based on electrochemical grafting technology. From 2003 to 2008, he was involved in the design of the BioMEA electrophysiological instrument dedicated for recording and stimulation on 256 Microelectrode array (MEA) for the neural networks studies. Since 2008, he has been the Project Manager of the electronic development for an active implantable medical device named WIMAGINE at CLINATEC, Grenoble, France.

Fabien Sauter-Starace received the Ph.D. degree in mechanics and material science in 2000.

He is currently a Project Manager and Research Engineer, and was previously a Senior Scientist at Corning FRC in the field of MEMS and BioMEMS design and packaging. From 2002 to 2008, he was in charge of several lab-on-chip and medical device projects at the CEA-LETI, such as the Neurolink project. He became an early member of CLINATEC, Grenoble, France, and is now in charge of the technological development concerning biocompatible packaging and microtechnologies.

Michael Foerster received his engineering degree from Ecole Centrale de Lyon, France, in 2008.

He gained his first experience in implantable devices within the Australian Vision Prosthesis Group. He is currently (since 2010) an Implantable Systems Engineer in the CLINATEC team, Grenoble, France, where his activities include system architecture specification, wireless and low power designs, embedded algorithms and neural stimulation.

David Ratel received the Ph.D. degree in neurosciences from Joseph Fourier University, Grenoble, France, in 2002.

After a postdoctoral fellowship at the Montreal Center for Experimental Therapeutics in Cancer, Montreal, Canada, he joined the CEA-LETI, Grenoble, in 2009, and is in charge of the biological evaluation of medical devices in CLINATEC.

Alim Louis Benabid received the medical degree in 1970 and Ph.D. degree in physics in 1978.

After a postdoctoral fellowship at the Salk Institute he was appointed Professor at Grenoble University, Grenoble, France, in Neurosurgery and Experimental Medicine until 1983, then in Neurosurgery and Biophysics. From 1988 to 2007, he was the Director of the research laboratory INSERM unit 318, entitled Preclinical Neurosciences, and from 1989 to 2007, Head of the Neurosurgery Department at the University Hospital of Grenoble, Professor of biophysics at Joseph Fourier University. He has centered his scientific activity on the approach of neurosurgical pathologies, particularly brain tumors and movement disorders, namely Parkinson's disease. He has designed a new method of stereotactic inhibition of surgical targets, namely deep brain stimulation (DBS) at high frequency. In 2007, he joined the French Commission of Atomic Energy as a Scientific Adviser and is Chairman of the Board of CLINATEC®.

Dr. Benabid is a member of the Institut Universitaire de France, of the French Academy of Sciences, of the French Academy of Medicine and of the Royal Academy of Medicine of Belgium, and he received a Doctorate Honoris Causa from the University of Galway, Ireland, from the University of London, Ontario, Canada, from McGill University, Montreal Quebec and from the University of Porto, Portugal.